Article published online: 2023-09-27

Research on the Effects of Neuroglobin on Ferroptosis in the Nerve Cells

Wenjin Gao[1] Chen Mo[1] Wei Feng[1] Xinmin Pan[1] Haojie Qin[1]

[1] School of Basic Medicine and Forensic Medicine, Henan University of Science and Technology, Luoyang, Henan, China

CMNP 2023;3:e133–e142.

Address for correspondence Haojie Qin, PhD, Associate Professor, School of Basic Medicine and Forensic Medicine, Henan University of Science and Technology, No. 263 Kaiyuan Avenue, Luoyang, Henan 471000, China (e-mail: herochin@haust.edu.cn).

Abstract

Objectives The objective of this article was to explore the effects of neuroglobin (NGB) on ferroptosis in the nerve cells.

Methods The NGB knockdown model of HT22 cells was constructed, and the ferroptosis-related indexes of cell proliferation activity, contents of iron ion, malondialdehyde (MDA), superoxide and reactive oxygen, and the changes of nuclear factor E2-related factor 2 (Nrf2) expression were examined in the normal group, erastin group, NGB siRNA group, and NGB siRNA + Erastin group, respectively.

Results Compared with the normal group, cell proliferation activity and Nrf2 expression were significantly lower in the erastin group, NGB siRNA group, and NGB siRNA + erastin group, and ferroptosis-related indexes such as iron ion content, MDA content, superoxide content, and reactive oxygen species content were significantly reduced, and the difference between NGB siRNA + erastin group, erastin group, and NGB siRNA group was statistically significant ($p < 0.05$).

Conclusion Knockdown of NGB in cells enhances the action of the ferroptosis inducer erastin, and NGB may regulate the cellular ferroptosis process through Nrf2. This research may provide references for the clinical treatment of nervous system disease with Chinese medicine.

Keywords
- neuroglobin
- HT22 cells
- ferroptosis
- siRNA
- nerve cells

Introduction

Neuroglobin (NGB) is a globulin mainly expressed in the cytoplasm of nerve cells. It has a neuroprotective effect in brain neurological disorders of ischemia, hypoxia and oxidative stress injury, stroke, and Alzheimer's disease (AD), and its protective effect may be related to stabilizing metal ion metabolism, scavenging reactive oxygen species (ROS), and reducing nitric oxide damage.[1–3] Cerebral hemorrhage belongs to the category of "stroke" in Chinese medicine. Studies have found that the higher the expression level of NGB protein in the brain tissue of patients with cerebral hemorrhage, the better the patient's condition.[4] Stroke in Chinese medicine is divided into meridian stroke and visceral stroke according to the state of mind of the stroke patients, and visceral stroke can be divided into obstruction syndrome and collapse syndrome according to the condition of the healthy qi and pathogenic factor. The expressions of NGB in yang obstruction, yin obstruction, and collapse syndrome of stroke are different, which is helpful for the syndrome differentiation and treatment of stroke.[4] Chinese medicine has a history of thousands of years and plays an important role in the prevention and treatment of diseases. Studies have found that many Chinese herbs, Chinese compound medicine, and monomer components of Chinese herbs can improve nerve cell damage by regulating the expression of NGB.[5,6] In addition, studies have demonstrated that overexpression of NGB can significantly attenuate H_2O_2-induced ROS/reactive nitrogen species accumulation and lipid peroxidation, reduce H_2O_2-induced mitochondrial dysfunction and apoptosis, which play a protective role against oxidative

received
March 20, 2023
accepted after revision
May 8, 2023

DOI https://doi.org/10.1055/s-0043-1773796.
ISSN 2096-918X.

© 2023. The Author(s).
This is an open access article published by Thieme under the terms of the Creative Commons Attribution License, permitting unrestricted use, distribution, and reproduction so long as the original work is properly cited. (https://creativecommons.org/licenses/by/4.0/)

Georg Thieme Verlag KG, Rüdigerstraße 14, 70469 Stuttgart, Germany

stress in nerve cells,[7] and polydatin can activate cAMP-response element-binding protein/NGB signaling pathway and protect neuron cells from hydrogen peroxide damage,[8] suggesting that NGB may participate in and improve the oxidative damage of nerve cells, and provide new insights for the research on the mechanism of Chinese medicine in improving the oxidative damage of nerve cells.

Studies have found that the upregulation of NGB expression can promote the survival of nerve cells under oxygen or glucose deprivation and oxidative stress. When the body is in a hypoxic state, the expression of NGB in cells increases rapidly, which is mainly mediated by hypoxia-inducible factor (HIF).[9,10] In 2012, Dixon et al[11] discovered ferroptosis when studying the mechanism of erastin (ferroptosis inducer) leading to the death of RAS mutant tumor cells. Ferroptosis is the regulatory cell death caused by the accumulation of lipid peroxide and ROS due to abnormal iron metabolism in cells. Studies have found that the main mechanism of ferroptosis is divided into three parts: iron metabolism, amino acid metabolism, and lipid peroxidation. When it is abnormal, it will lead to cell membrane rupture and even death.[12–14] It has been confirmed that ferroptosis is involved in neurodegeneration such as brain stroke, traumatic brain injury, and AD.[15–17] Studies have shown that HIF can participate in the process of ferroptosis by regulating the expression of metabolism of iron ions in vivo, glutathione (GSH) peroxidase 4 (GPX4)-related amino acids, and polyunsaturated fatty acids (PUFA).[18–27] In view of the relationship between ferroptosis and HIF, HIF and NGB, and the neuroprotective mechanism of NGB, it is speculated that NGB may participate in cell ferroptosis and improve oxidative damage. Studies have found that the overexpression of NGB can significantly enhance the resistance of human neuroblastoma cells SH-SY5Y to ferroptosis inducers and can effectively protect cells from ferroptosis injury.[28] Nuclear factor E2-related factor 2 (Nrf2) is a kind of basic leucine zipper (bZIP) transcription factor with anti-oxidative stress effect and it can bind with multiple proteins in cells to exert coregulation effects on multiple genes. Nrf2 is involved in the regulation of various proteins related to iron ion metabolism and can also act on the cystine-glutamate antitransport system and GPX4.[29] NGB is also involved in the cystine-glutamate antitransport system.[30] Based on the above studies, this experiment constructed the NGB knockdown model of mouse hippocampal neuron HT22 and explored the possible role of NGB in neuronal ferroptosis by examining the changes in related indicators and Nrf2 expression after erastin-induced ferroptosis when NGB was knocked down.

Material

Cells

Mouse hippocampal neuron cells (HT22) were donated by West China Second Hospital of Sichuan University.

Drugs and Reagents

Following drugs and reagents were used: NGB siRNA (Target sequence 5′-ATGGCGCTGCATGTGCGTTGA-3′, Bioengineering [Shanghai] Co., Ltd.); LipoRNAi transfection reagent, HRP-goat anti-rabbit IgG, FITC-labeled goat anti-rabbit IgG (H + L), DAPI staining solution, ROS detection kit, superoxide anion fluorescence probe (Shanghai Biyuntian Biotechnology Co., Ltd., No.: C0535, A0208, A0562, C1005, S0033s, S0063); BCA protein quantification kit (Kangwei Century Biotechnology Co., Ltd., No.: CW0014S); anti-NGB polyclonal antibody, CCK-8 reagent, and tissue iron content detection kit (Beijing Solaibao Technology Co., Ltd., No.: K004560P, C0038, BC4355); erastin (Shanghai McLin Biochemical Technology Co., Ltd., No.: E872563); cell malondialdehyde (MDA) determination kit (Nanjing Jiancheng Institute of Bioengineering, No.: A0034-1).

Instruments

Instruments used were as follows: tri-gas incubator (Thermo Fisher SCIENTIFIC, No.: 50163013); full wavelength microplate reader (Thermo Fisher SCIENTIFIC,No.: 1510); inverted phase contrast microscope (Leica, No.: DFC7000 T); protein electrophoresis system (BIO RAD, No.: 041BR170811); biosafety cabinet (AIRTECH Sujing Antai, No.: BSC-1304IIIA2).

Methods

Cell Culture and Grouping

HT22 cells were cultured in Dulbecco's Modified Eagle Medium containing 10% fetal bovine serum and 1×10^5U/L penicillin-streptomycin under the condition of 37°C and 5% CO_2. When the confluence of the cells in the culture flask reached 80 to 90%, the cells were subcultured and the cells in the logarithmic growth phase were used for experiments. The HT22 cells were divided into normal group, LipoRNAi group, erastin group, NGBsiRNA interference group and NGBsiRNA + erastin group. Cells in the normal group were cultured as described above; cells in the LipoRNAi group were cultured in the above manner until the confluence of the cells reached 70 to 80% and, then, replaced with the basal medium containing the corresponding volume of LipoRNAi; cells in the erastin group were cultured as above and replaced with erastin-containing medium (the final concentration of erastin was 20 μmol/L) at corresponding time. In the NGBsiRNA interference group, when the confluence of the cells reached 70 to 80%, they were transfected according to the kit instructions. After transfection, the NGBsiRNA interference group continued to culture as above, while the cells in the NGBsiRNA + erastin group were replaced with erastin-containing medium (the final concentration of erastin was 20 μmol/L) 24 hours after transfection.

Detection of Neuroglobin Expression Level in Cells

HT22 cells were inoculated at 1.5×10^5 cells/well in a 6-well plate with a clean cover glass, fixed with 4% paraformaldehyde when the confluence of the cells reached 70 to 80%, and Triton-X100 was used to rupture the membrane. Five percent goat serum was used as block solution, NGB polyclonal antibody (1:50 dilution ratio) was added and incubated overnight at 4°C, and goat antirabbit FITC fluorescent secondary antibody (1:600 dilution ratio) was added and incubated at room

temperature in the dark for 1 hours and then incubated with DAPI solution at room temperature for 5 minutes; the negative control phosphate-buffered saline (PBS) was used to replace the primary antibody, and the expression of NGB in the cells was observed under an inverted phase-contrast fluorescence microscope and photographed. The cells in the normal group and the NGB siRNA interference group were transfected with NGB siRNA for 48 hours to extract the total cell protein. Protein concentration was determined using the BCA method. Equal amounts of protein samples were mixed with 5× protein loading buffer at a 4:1 ratio and then subjected to boiling water for 10 minutes to denature the proteins. Subsequently, with a 12% separating gel and a 5% stacking gel in place, the protein samples were sequentially loaded into the sample wells. A constant voltage of 80 V was maintained until the indicator reached the junction of the stacking gel and the separating gel. At this point, the voltage was increased to 100 V for the duration of constant voltage electrophoresis. A polyvinylidene difluoride (PVDF) membrane of 0.22 μm was cut of the same size as the gel and activated in methanol for 10 minutes. Gel and PVDF membrane were placed in the order of cathode to anode, that is, sponge pad–filter paper–gel–PVDF membrane–filter paper–sponge pad, and were rotated at a constant current of 200 mA for 45 minutes. The PVDF membrane was blocked for 1 hour at 37°C in a shaker and washed. NGB (dilution ratio 1:1,000) and beta actin (dilution ratio 1:2,000) were added for incubation in a shaker at 4°C overnight, and the membrane was washed. HRP-labeled goat antirabbit secondary antibody (dilution ratio 1:1,000) was added for incubation in a shaker at room temperature for 1 hour and the membrane was washed. ECL luminescence reagent solution A and solution B were mixed in equal proportions and added dropwise on the PVDF membrane and incubated at room temperature for 3 minutes, and the results were observed in a gel imager, the expression of NGB protein was recorded by taking pictures, and the protein was semiquantitatively analyzed using Image J software.

Detection of Cell Proliferation Activity by the CCK-8 Method

HT22 cells were inoculated in 96-well plates at 1×10^4-cells/well, and six replicate wells were set up in each group. Grouping was performed. After incubating in the incubator for 4 hours, the complete medium was used, culturing for 2 hours. Finally, CCK-8 working solution was added, and after incubation in the incubator for 0.5 hours, the absorbance value was detected at 450 nm with a microplate reader, and the measurement was repeated three times.

Detection of Iron Ion Content

HT22 cells were inoculated in 12-well plates at 1.2×10^5 cells/well, and six replicate wells were set up in each group. After being grouped by the method mentioned before, culture continued for 24 hours, cell protein was extracted, and BCA protein concentration was detected. The configuration of the blank tube, standard tube, and test tube reagents followed the instructions provided in the kit. The mixture was placed in a water bath at 100°C for 5 minutes and then cooled with tap water. Subsequently, 60 μL of chloroform was added to each tube, thoroughly mixed, and then centrifuged at 10,000 $r \cdot min^{-1}$ for 10 minutes. Following centrifugation, 200 μL of the upper inorganic phase was transferred to a 96-well plate. Finally, the absorbance at 520 nm was measured using a microplate reader preheated to 37°C, and the iron content for each sample group was calculated.

Malondialdehyde Content Detection

HT22 cells were inoculated in 12-well plates at 1.2×10^5 cells/well, and six replicate wells were set up in each group. After being grouped by the method mentioned before, culture continued for 24 hours, cell protein was extracted, and BCA protein concentration was detected. Complete blank tube, standard tube, and measurement tube reagent configuration were used according to the kit instructions. Each tube was heated in a water bath above 95°C for 40 minutes, cooled under running water, and centrifuged at 4,000 $r \cdot min^{-1}$ for 10 minutes, and 250 μL of the reaction solution of each tube was pipetted into a 96-well plate, the absorbance value was measured at 530 nm using a microplate reader, and MDA content of each group of samples was calculated.

Superoxide Detection

Cells were inoculated in 6-well plates at 1.5×10^5 cells/well, and three replicate wells were set up in each group. After being grouped by the method mentioned before, the cells were cultured for 4 hours and then replaced with superanion probe working solution (5 mmol/L), 2 mL per well, incubated in an incubator for 30 minutes, washed twice with PBS, and observed and photographed under an inverted fluorescent microscope.

Active Oxygen Detection

Cells were inoculated in 6-well plates at 1.5×10^5 cells/well, and three replicate wells were set up in each group. Following the previously mentioned grouping method, the cells were cultured for 4 hours. Afterward, they were subjected to the DCFH-DA working solution (prepared by diluting the DCFH-DA stock solution with basic culture medium at a ratio of 1:1,000), with 2 mL added per well. The cells were then incubated in a controlled environment for 20 minutes, washed twice with PBS, and subsequently observed and photographed under an inverted fluorescent microscope.

Detection of Nuclear Factor E2-Related Factor 2 Protein Expression

Cells were seeded in 6-well plates at 1.5×10^5 cells/well, and three replicate wells were set up in each group. Cell proteins were extracted 24 hours after adding Erastin, and BCA protein concentration was detected to prepare 10% separating gel and 5% stacking gel. An equal amount of protein sample was taken, mixed with 5× protein loading buffer in a ratio of 4:1boiled in water for 10 minutes to denature the protein, added well sequentially to the sample, and kept at the voltage constant of 80 V. When the indicator reached the junction of the stacking gel and the separating gel, the voltage was

 © 2023. The Author(s).

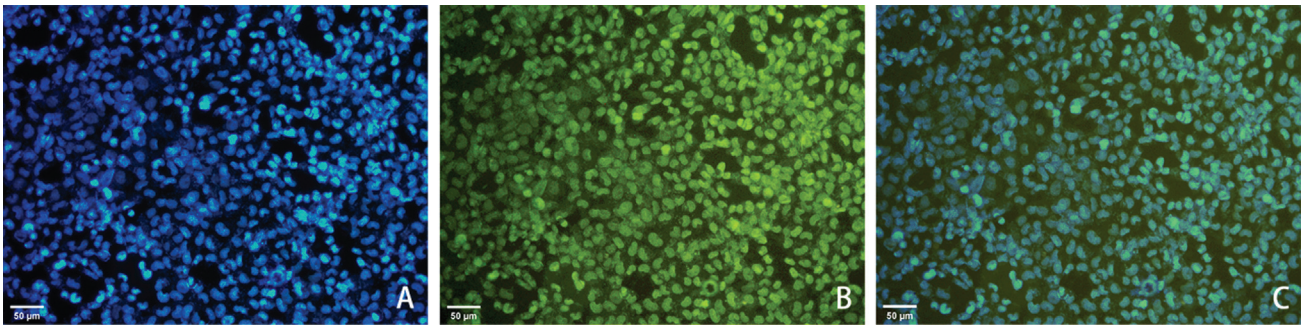

Fig. 1 Expression of NGB in HT22. Notes: (**A**) DAPI staining; (**B**) NGB expression; (**C**) merge map; ×200.

increased to 100 V for constant voltage electrophoresis. The PVDF membrane with a pore size of 0.45 μm was cut to match the dimensions of the gel and then activated in methanol for 10 minutes.

Gel and PVDF membrane were placed in the order of cathode to anode, that is, sponge pad–filter paper–gel–PVDF membrane–filter paper–sponge pad, and were rotated at a constant current of 200 mA for 1 hour and 20 minutes. The PVDF membrane was sealed for 1 hour at 37°C in a shaker and washed. Nrf2 (1:1,000 dilution ratio) and beta actin (1:2,000 dilution ratio) were added for incubation in a shaker at 4°C overnight, and the membrane was washed. HRP-labeled goat antirabbit secondary antibody (1:1,000 dilution ratio) was added at the room temperature for 1 hour and the membrane was washed. ECL luminescent reagent solution A and solution B were mixed in equal proportions and dropped on the PVDF membrane, incubated at room temperature for 3 minutes; then, the results were observed in a gel imager and the expression of Nrf2 protein was recorded by taking pictures, and the protein was semiquantitatively analyzed using Image J software.

Statistical Analysis

Data analysis was performed using GraphPad Prism 9 software, and the data were expressed as mean ± standard deviation ($\bar{x} \pm s$). The *t*-test was used for pairwise comparison between groups, and one way analysis of variance was used for data comparison among multiple groups. $p < 0.05$ indicates that the difference is statistically significant.

Results

Detection Results of Neuroglobin Expression Level in HT22 Cells

Cell immunofluorescence results showed that NGB was expressed in HT22 cells (►**Fig. 1**); compared with the normal group, after NGB siRNA interference, the expression of NGB in HT22 cells in the NGB siRNA interference group was significantly reduced ($p < 0.05$; ►**Fig. 2**).

Detection Results of CCK-8 Cell Proliferation Activity

Compared with the normal group, the cell proliferation activity of erastin group, NGB siRNA group, and NGBsiRNA + erastin group was significantly decreased ($p < 0.05$). There was no significant difference in cell proliferation activity between the erastin group and NGB siRNA group ($p > 0.05$); compared with cells in the erastin group and NGB siRNA group, the proliferation activity of cells in erastin + NGB siRNA group was significantly decreased ($p < 0.05$; ►**Fig. 3**).

Detection Results of Cellular Iron Ion Content

Compared with the normal group, the iron ion contents in the cells of the erastin group, the NGB siRNA group, and the NGBsiRNA + erastin group were all significantly increased

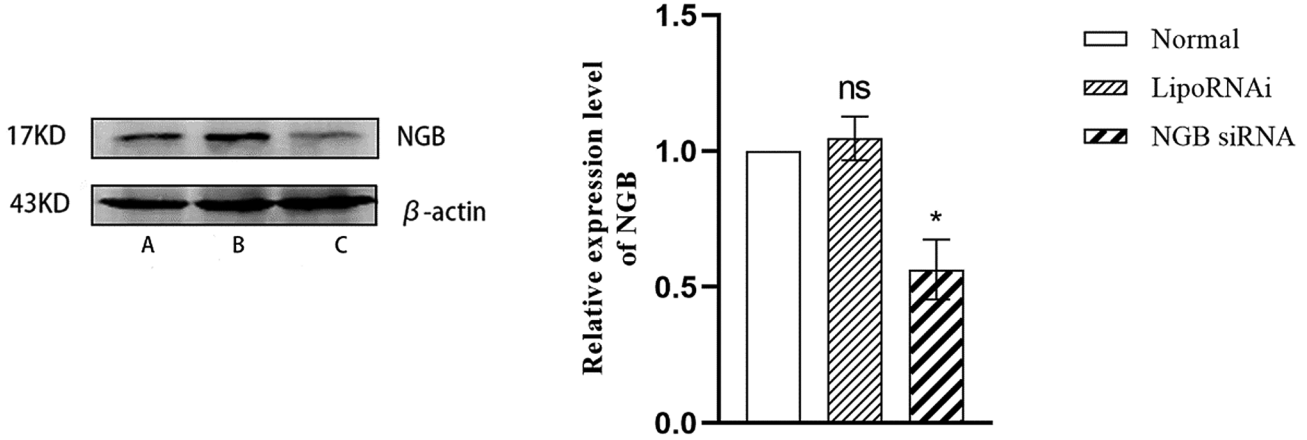

Fig. 2 Comparison of NGB protein expression levels in HT22 cells in each group. Notes: (**A**) normal group. (**B**) LipoRNAi group. (**C**) NGB siRNA interference group; * $p < 0.05$.

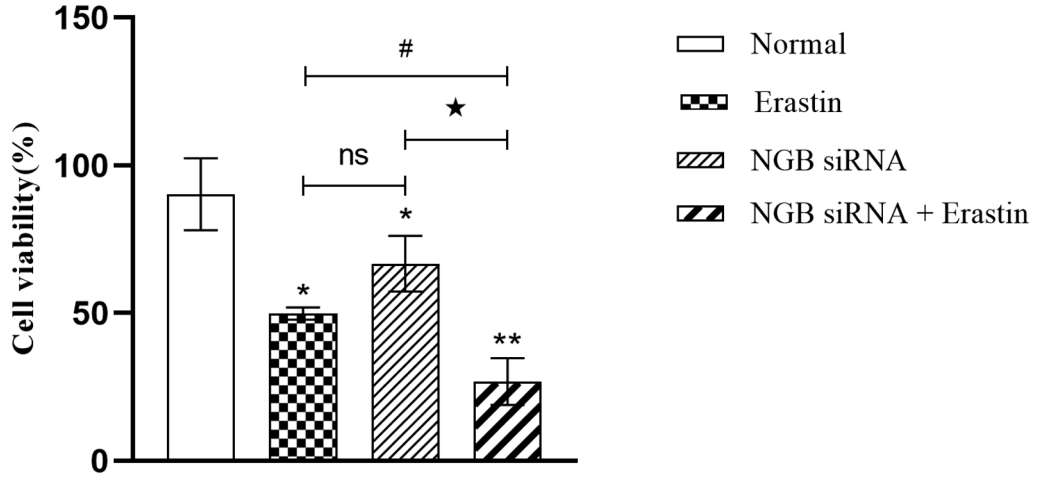

Fig. 3 Comparison of HT22 cell viability in each group. Notes: Compared with the normal group, $^{*}p < 0.05$, $^{**}p < 0.01$; compared to the erastin group, $^{\#}p < 0.05$, $^{\#\#}p < 0.01$; compared with the NGB siRNA group,$\bigstar p < 0.05$,$\bigstar\bigstar p < 0.01$.

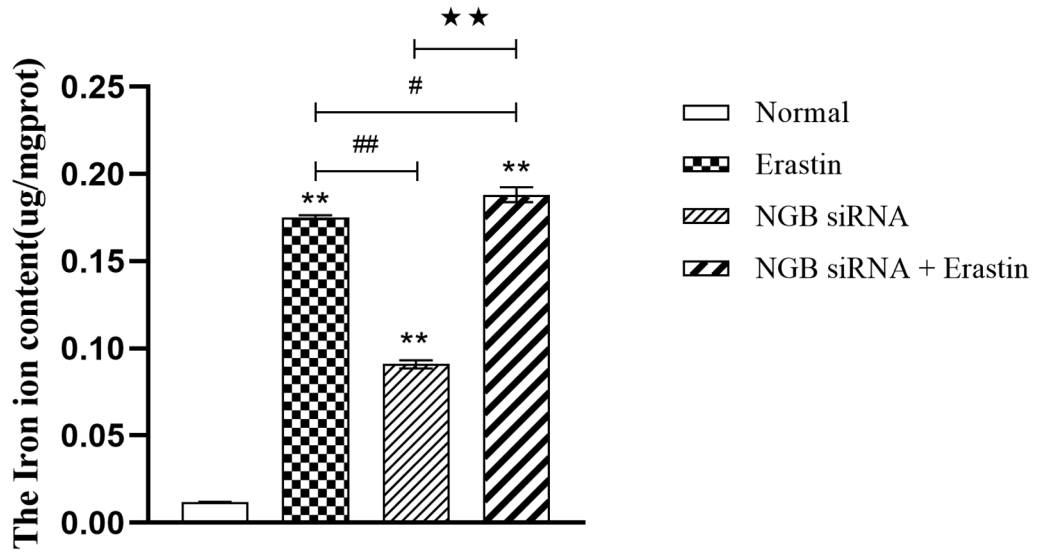

Fig. 4 Comparison of iron ion contents in HT22 cells in each group. Notes: Compared with the normal group, $^{*}p < 0.05$, $^{**}p < 0.01$; compared to the erastin group, $^{\#}p < 0.05$, $^{\#\#}p < 0.01$; compared with the NGB siRNA group, $\bigstar p < 0.05$,$\bigstar\bigstar p < 0.01$.

($p < 0.05$). Compared with the erastin group and NGB siRNA group, the intracellular iron ion content of NGBsiRNA + erastin group increased ($p < 0.05$; ►**Fig. 4**).

Malondialdehyde Content Detection Results

Compared with the normal group, the MDA content in cells of Erastin group, NGB siRNA group and NGBsiRNA + Erastin group were all significantly increased ($p < 0.05$); Compared with Erastin group and NGB siRNA group, the MDA content in cells of NGBsiRNA + Erastin group was significantly increased ($p < 0.05$; ►**Fig. 5**).

Detection Results of Superoxide Content

Compared with the normal group, the superoxide content in the cells of the erastin group, the NGB siRNA group, and the NGBsiRNA + erastin group were all significantly increased ($p < 0.05$). Compared with the erastin group and NGB siRNA group, the superoxide content in cells of NGBsiRNA + erastin group was significantly increased ($p < 0.05$; ►**Figs. 6** and **7**).

Detection Results of Cellular Active Oxygen Content

Compared with the normal group, the content of ROS in the erastin group, NGB siRNA group, and NGB siRNA + erastin group was significantly increased ($p < 0.01$). Compared with the erastin group and NGB siRNA group, the content of reactive oxygen in cells of NGB siRNA + erastin group was significantly increased ($p < 0.01$; ►**Figs. 8** and **9**).

Nuclear Factor E2-Related Factor 2 Protein Expression Detection Results

Compared with the normal group, the expression of Nrf2 protein in the erastin group, NGB siRNA group, NGB siRNA + erastin group was significantly decreased ($p < 0.05$). Compared with the erastin group, there was no significant

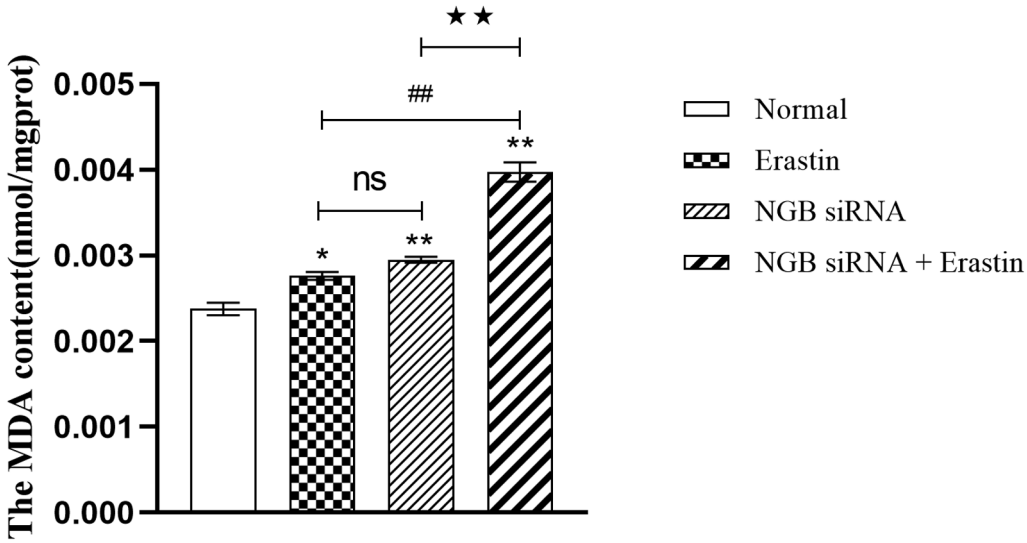

Fig. 5 Comparison of MDA content in HT22 cells in each group. Notes: Compared with the normal group, $^{*}p < 0.05$, $^{**}p < 0.01$; compared with the erastin group, $^{\#}p < 0.05$, $^{\#\#}p < 0.01$; compared with the NGB siRNA group, $^{\bigstar}p < 0.05$, $^{\bigstar\bigstar}p < 0.01$.

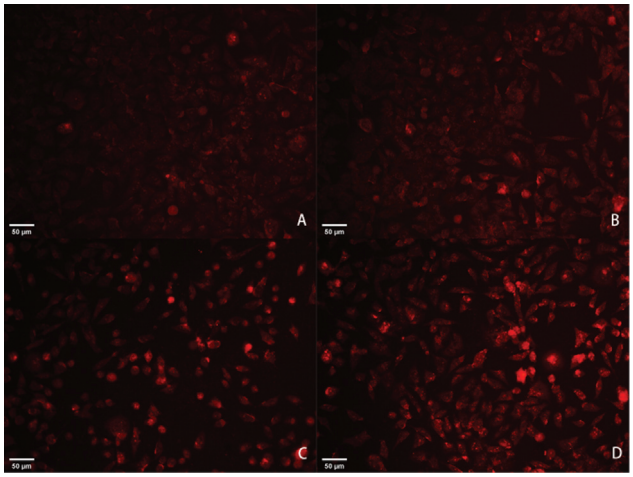

Fig. 6 Detection of superoxide content in HT22 cells in each group under light microscope. Notes: (**A**) normal group; (**B**) erastin group; (**C**) NGB siRNA interference group; (**D**) NGB siRNA + erastin group; ×200.

difference in Nrf2 protein expression in the NGB siRNA group ($p > 0.05$). Compared with the NGB siRNA group and erastin group, the expression of histone Nrf2 in NGB siRNA + erastin group was significantly decreased ($p < 0.01$; ►**Fig. 10**).

Discussion

When ferroptosis occurs in cells, the main morphological manifestations are cell membrane rupture, blebbing, reduction of mitochondrial cristae, mitochondrial miniaturization, and chromatin noncondensation.[31] In the process of iron ion metabolism, proteins related to iron absorption and transport, such as transferrin (Tf), transferrin receptor (TfR), and divalent metal transporter 1(DMT1),[14] proteins related to iron storage such as ferritin,[32] and proteins related to iron export, such as iron transporter (ferroportin, Fpn),[33] are abnormally expressed and lead to abnormal accumulation of iron, resulting in cellular ferroptosis. In terms of amino acid metabolism, ferroptosis is mainly related to GPX4.[34] GPX4 is the key enzyme of the important antioxidant system in the human body, which can convert lipid peroxide (ROOH) into nontoxic steroidal alcohol (ROH); thereby, it resists the damage of lipid peroxidation products and ROS to the biomembrane[35] and its antioxidant effect depends on GSH, and the intracellular cystine-glutamate antitransport system is mainly responsible for the synthesis of GSH and further synthesizes GSH by ingesting extracellular cystine and transferring the intracellular toxic glutamate.[36] Erastin, a commonly used ferroptosis inducer, acts on the cystine-glutamate antitransport system to cause ferroptosis.[37] PUFA provide the molecular basis for the fluidity and deformability of the cell membrane lipid bilayer structure. Due to the presence of carbon–carbon double bonds on PUFA, PUFA in the cell and free radicals will generate peroxidation reaction, which will become the target of ferroptosis.[38] When ferroptosis occurs in cells, there will be abnormal accumulation of iron to generate a large amount of ROS, which then reacts with PUFAs to destroy the cell membrane structure and lead to cell death. The above process is accompanied by changes in iron ion content, MDA content, superoxide content, and ROS content, which can be used as the detection index of ferroptosis.

This experiment found that after adding the ferroptosis inducer erastin, the cell proliferation activity decreased, and the contents of cellular iron ions, MDA, superoxide, and cellular ROS increased, indicating that the ferroptosis model of HT22 cells was successfully established. After the knockdown of NGB, the cell proliferation activity decreased, and the contents of cellular iron ion, MDA, and superoxide increased. After the knockdown of NGB, the ferroptosis inducer erastin was added, and the cell proliferation activity was further reduced, and the contents of cellular iron ions, MDA, superoxide, and cellular ROS were significantly increased. The above results indicate that the knockdown of NGB can enhance the effect of erastin and promote ferroptosis.

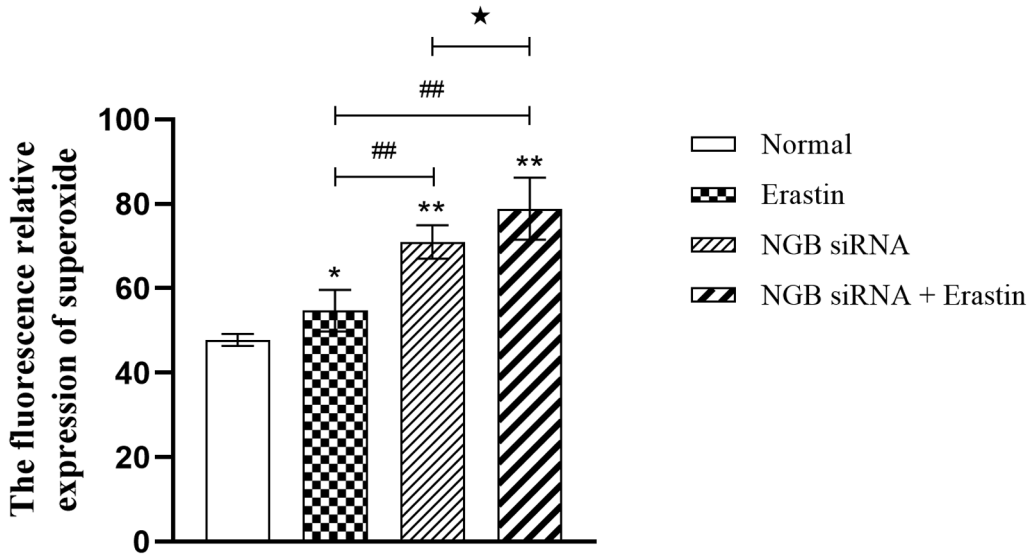

Fig. 7 Comparison of superoxide content in HT22 cells in each group. Notes: Compared with the normal group, $^{*}p < 0.05$, $^{**}p < 0.01$; compared with the erastin group, $^{\#}p < 0.05$, $^{\#\#}p < 0.01$; compared with the NGB siRNA group, $\bigstar p < 0.05$, $\bigstar\bigstar p < 0.01$.

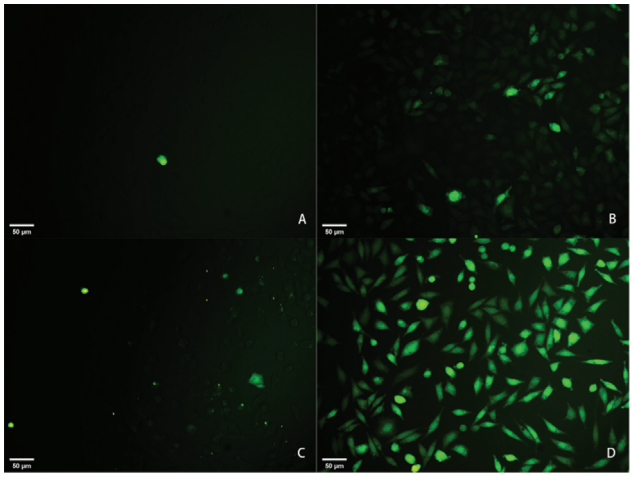

Fig. 8 Detecting the content of reactive oxygen in HT22 cells in each group under light microscope. Notes: (**A**) normal group; (**B**) erastin group; (**C**) NGB siRNA interference group; and (**D**) NGB siRNA + erastin group; ×200.

NGB has the function of protecting nerve cells when cranial nerve cells suffer from ischemic hypoxic injury, brain contusion, cerebral hemorrhage, or AD diseases. Studies found that in the mouse model of middle cerebral artery occlusion, NGB overexpression effectively reduced the size of cerebral ischemic infarction,[39] and in the rat model of global cerebral ischemia, limb ischemic preconditioning, the expression of NGB increased, which effectively alleviated the damage of nerve cells caused by ischemia and reperfusion. At the same time, it was also found that the expression level of NGB in the hippocampus, cortex, and hypothalamus was positively correlated with the time of ischemia and reperfusion.[40] In the research on AD, it was found that NGB was related to the characteristic changes of AD, such as β-amyloid deposition, hyperphosphorylation of tau protein.[41] Simultaneously, the damage caused by β-amyloid deposition in PC12 cells with NGB transfection overexpression was alleviated.[42] Xu et al[43] found that 50-Hz high-frequency electroacupuncture stimulation had a better therapeutic effect on cerebral hemorrhage rats than 2 and 15-Hz low-frequency electroacupuncture stimulation, and its therapeutic mechanism may be related to the regulation of NGB expression in hematoma brain tissue. Bushen Yisui decoction combined with acupuncture can significantly increase serum NGB levels in patients with mild cognitive impairment after cerebral infarction and can significantly increase blood flow in ischemic sites and improve cognitive function in patients.[44] Tongdu Tiaoshen acupuncture can effectively increase the level of serum NGB in patients with postischemic stroke cognitive impairment on the basis of conventional Western medicine treatment, thereby improving the clinical symptoms of patients.[45] The expression of NGB is up-regulated in rats with septic encephalopathy. Electroacupuncture at Baihui (DU 20) and Shuigou (DU 26) in rats has a therapeutic effect on septic encephalopathy, and the effect is most obvious after 24 hours. The action mechanism is related to the up-regulation of NGB expression.[46] Yan et al[47] found that acupuncture at Dazhui (DU 14), Baihui(GV 20), and Renzhong (DU 26) could up-regulate the expression level of NGB in the hippocampus of rats after cerebral ischemia–reperfusion injury, thereby achieving brain protection. In an ischemic stroke model, it was found that NGB could effectively remove ROS biomarkers and played a neuroprotective role by combining NO and H_2O_2.[48,49] Other studies have shown that NGB might exert the ability to remove active substances through the combination of histidine and ROS or through the interaction among the proteins in the respiratory chain.[50,51] Based on the above and the results of this experiment, it is speculated that NGB protects neurons not only by acting against cell necrosis and apoptosis[2] but also by inhibiting ferroptosis.

Nrf2 is a key transcription factor that maintains redox balance and normal signal transduction in the human body.[52] The six highly conservative functional structure

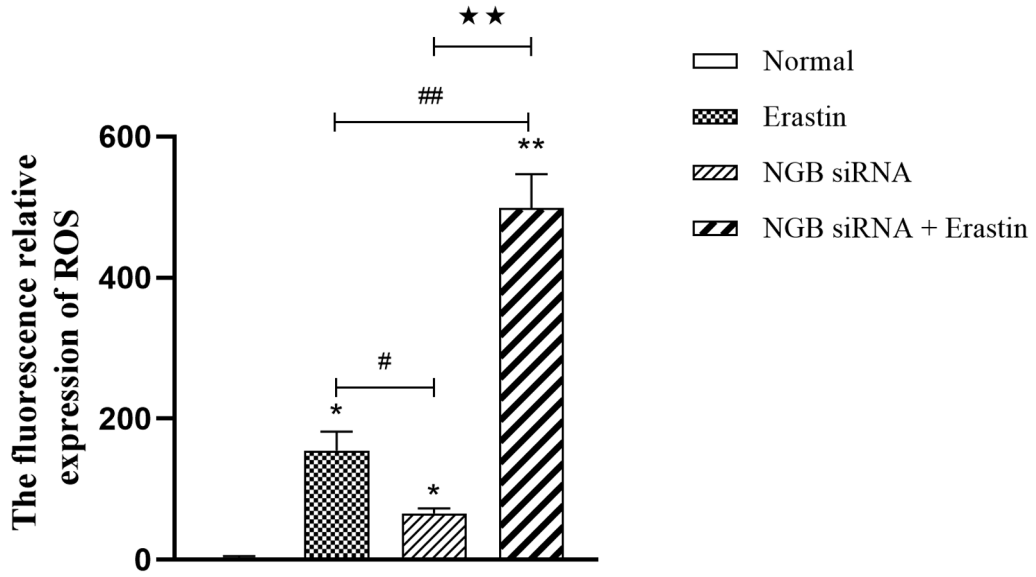

Fig. 9 Comparison of active oxygen content in HT22 cells in each group. Notes: Compared with the normal group, $^{*}p < 0.05$, $^{**}p < 0.01$; compared with the erastin group, $^{\#}p < 0.05$, $^{\#\#}p < 0.01$; compared with the NGB siRNA group, $\bigstar p < 0.05$, $\bigstar\bigstar p < 0.01$.

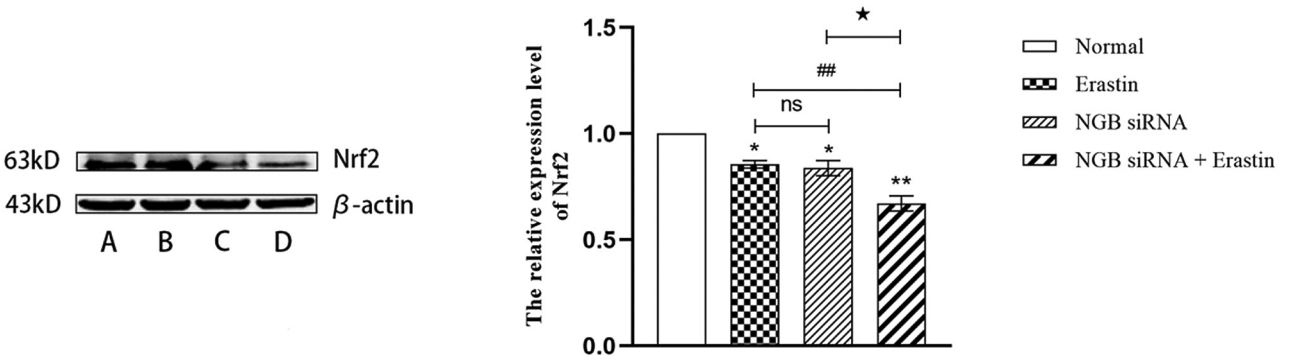

Fig. 10 Comparison of the relative expression of Nrf2 in HT22 cells in each group. Notes: (**A**) normal group; (**B**) erastin group; (**C**) NGB siRNA interference group; (**D**) NGB siRNA + erastin group; compared with the normal group, $^{*}p < 0.05$, $^{**}p < 0.01$; compared with the erastin group, $^{\#}p < 0.05$, $^{\#\#}p < 0.01$; compared with the NGB siRNA group, $\bigstar p < 0.05$, $\bigstar\bigstar p < 0.01$.

regions (Neh1–Neh6) can maintain the stability of their own structures and functions and also regulate the expression of related downstream molecules at the transcription level.[48] Studies have found that Jinzhan Yinpan (Bidens Biternata) could effectively improve carbon tetrachloride-induced acute liver injury, and the action mechanism was related to the activation of Nrf2/Keap1 signaling pathway to inhibit oxidative stress injury.[53] Liuwei Dihuang pill has a significant protective effect on oxidative stress in AD model cells, and its mechanism may be achieved by regulating the expression of antioxidant factors in the Nrf2/HO-1 pathway.[54] This experiment found that after NGB expression was knocked down, the expression of Nrf2 in cells decreased, and on the basis of NGB knockdown, erastin could further reduce the expression of Nrf2, indicating that the change of NGB expression can cause the change of Nrf2 expression, and NGB knockdown can enhance the effect of ferroptosis inducer erastin. It is speculated that NGB and Nrf2 might be related to some pathways in the mechanism of ferroptosis. Studies have found that NGB could protect nerves by stabilizing the combination of HIF and DNA, and Nrf2 and DNA. At the same time, NGB could also prevent the abnormal release of iron through HIF and Nrf2 and reduce cell death.[10] The steroid hormone 17 β-estradiol (E2) could play an antioxidative stress role through NGB, and in NGB knockout cells, E2's ability to regulate Nrf2 was weakened.[55] When studying its neuroprotective effect by constructing manganese porphyrin recombinant metalloprotein (Mn-TAT-PTD-NGB), it was also found that it could effectively clear ROS and restore mitochondrial function. The expressions of Nrf2, superoxide dismutase (SOD), and catalase(CAT) all increased, suggesting that NGB might participate in the body's antioxidative stress process by regulating Nrf2.[56,57]

Conclusion

Knockdown of NGB can enhance the effect of iron death inducer erastin and thus promote the occurrence of ferroptosis, and NGB may participate in the process of cell ferroptosis by regulating Nrf2. This study provides a reference for

exploring the mechanism of Chinese medicine to improve the oxidative damage of nerve cells and provides new strategies and inspiration for the clinical application of Chinese medicine in the treatment of neurological diseases. However, due to the complexity of cell injury mechanisms and metabolic pathways, the specific mechanism of NGB involved in the protection of nerve cells against iron death still needs to be further studied.

CRediT Authorship Contribution Statement

W.G. was responsible for data curation, visualization, software, and writing—original draft. C.M. was responsible for conceptualization, data curation, formal analysis, and writing—original draft. W.F. was responsible for investigation, data curation, and project administration. X.P. was responsible for writing—review and editing and formal analysis. H.Q. was responsible for conceptualization, methodology, funding acquisition, supervision, and writing-review & editing.

Funding

This work was funded by Henan Science and Technology Research Program Project (222102310398).

Conflict of Interest

The authors declare no conflict of interest.

References

1 Blanco S, Martínez-Lara E, Siles E, Peinado MÁ New strategies for stroke therapy: nanoencapsulated neuroglobin. Pharmaceutics 2022;14(08):1737
2 Fiocchetti M, Cracco P, Montalesi E, Fernandez VS, Stuart JA, Marino M. Neuroglobin and mitochondria: The impact on neurodegenerative diseases. Arch Biochem Biophys 2021;701:108823
3 De Simone G, Sbardella D, Oddone F, Pesce A, Coletta M, Ascenzi P. Structural and (pseudo-) enzymatic properties of neuroglobin: its possible role in neuroprotection. Cells 2021;10(12):3366
4 Ma DM. Expression of NGB of Brain Tissue Around Hematoma in Patients with Cerebral Hemorrhage and Its Relationship with Obstruction Syndrome and Collapse Syndrome in Chinese Medicine. Fuzhou: Gujian College of Chinese Medicine
5 Yang H. Protective Effects of Juema (Potentilla anserina L.) and Its Effects on the Expression of Neuroglobin. Shijiazhuang: Hebei Medical University
6 Zheng SM, Lin XF, Yang L, et al. Protective effects of Senkyunolidelon rats with septic encephalopathy based on the signal path of p38 MAPK. Tradit Chin Drug Res Pharmacol 2019;30(09): 1083–1087
7 Li RC, Morris MW, Lee SK, Pouranfar F, Wang Y, Gozal D. Neuroglobin protects PC12 cells against oxidative stress. Brain Res 2008; 1190:159–166
8 Zhang H, Li Y, Xun Y, et al. Polydatin protects neuronal cells from hydrogen peroxide damage by activating CREB/Ngb signaling. Mol Med Rep 2022;25(01):9
9 Liu A, Brittain T. A futile redox cycle involving neuroglobin observed at physiological temperature. Int J Mol Sci 2015;16 (08):20082–20094
10 Hota KB, Hota SK, Srivastava RB, Singh SB. Neuroglobin regulates hypoxic response of neuronal cells through Hif-1α- and Nrf2-mediated mechanism. J Cereb Blood Flow Metab 2012;32(06):1046–1060
11 Dixon SJ, Lemberg KM, Lamprecht MR, et al. Ferroptosis: an iron-dependent form of nonapoptotic cell death. Cell 2012;149(05): 1060–1072
12 Bogdan AR, Miyazawa M, Hashimoto K, Tsuji Y. Regulators of iron homeostasis: new players in metabolism, cell death, and disease. Trends Biochem Sci 2016;41(03):274–286
13 Yu H, Guo P, Xie X, Wang Y, Chen G. Ferroptosis, a new form of cell death, and its relationships with tumourous diseases. J Cell Mol Med 2017;21(04):648–657
14 Chen X, Li D, Sun HY, et al. Relieving ferroptosis may partially reverse neurodegeneration of the auditory cortex. FEBS J 2020; 287(21):4747–4766
15 Cui Y, Zhang Y, Zhao X, et al. ACSL4 exacerbates ischemic stroke by promoting ferroptosis-induced brain injury and neuroinflammation. Brain Behav Immun 2021;93:312–321
16 Wehn AC, Khalin I, Duering M, et al. RIPK1 or RIPK3 deletion prevents progressive neuronal cell death and improves memory function after traumatic brain injury. Acta Neuropathol Commun 2021;9(01):138
17 Wang ZL, Yuan L, Li W, Li JY. Ferroptosis in Parkinson's disease: glia-neuron crosstalk. Trends Mol Med 2022;28(04):258–269
18 Xu M, Tan X, Li N, et al. Differential regulation of estrogen in iron metabolism in astrocytes and neurons. J Cell Physiol 2019;234 (04):4232–4242
19 Schwartz AJ, Das NK, Ramakrishnan SK, et al. Hepatic hepcidin/intestinal HIF-2α axis maintains iron absorption during iron deficiency and overload. J Clin Invest 2019;129(01):336–348
20 Schwartz AJ, Converso-Baran K, Michele DE, Shah YM. A genetic mouse model of severe iron deficiency anemia reveals tissue-specific transcriptional stress responses and cardiac remodeling. J Biol Chem 2019;294(41):14991–15002
21 Wu Y, Zhang S, Gong X, et al. The epigenetic regulators and metabolic changes in ferroptosis-associated cancer progression. Mol Cancer 2020;19(01):39
22 Zou Y, Palte MJ, Deik AA, et al. A GPX4-dependent cancer cell state underlies the clear-cell morphology and confers sensitivity to ferroptosis. Nat Commun 2019;10(01):1617
23 Friedmann Angeli JP, Krysko DV, Conrad M. Ferroptosis at the crossroads of cancer-acquired drug resistance and immune evasion. Nat Rev Cancer 2019;19(07):405–414
24 Chen J, Chen J, Fu H, et al. Hypoxia exacerbates nonalcoholic fatty liver disease via the HIF-2α/PPARα pathway. Am J Physiol Endocrinol Metab 2019;317(04):E710–E722
25 Venkatesh D, O'Brien NA, Zandkarimi F, et al. MDM2 and MDMX promote ferroptosis by PPARα-mediated lipid remodeling. Genes Dev 2020;34(7-8):526–543
26 Ratan RR. The chemical biology of ferroptosis in the central nervous system. Cell Chem Biol 2020;27(05):479–498
27 Rroji O, Kumar A, Karuppagounder SS, Ratan RR. Epigenetic regulators of neuronal ferroptosis identify novel therapeutics for neurological diseases: HDACs, transglutaminases, and HIF prolyl hydroxylases. Neurobiol Dis 2021;147:105145
28 Van Acker ZP, Van Raemdonck GA, Logie E, et al. Connecting the dots in the neuroglobin-protein interaction network of an unstressed and ferroptotic cell death neuroblastoma model. Cells 2019;8(08):873
29 Imai H, Matsuoka M, Kumagai T, et al. Lipid Peroxidation-Dependent Cell Death Regulated by GPx4 and Ferroptosis//Current Topics in Microbiology and Immunology. Cham: Springer International Publishing; 2016:143–170
30 Guo Y, Yuan H, Jiang L, et al. Involvement of decreased neuroglobin protein level in cognitive dysfunction induced by 1-bromopropane in rats. Brain Res 2015;1600:1–16
31 Xie Y, Hou W, Song X, et al. Ferroptosis: process and function. Cell Death Differ 2016;23(03):369–379
32 Torti SV, Torti FM. Iron and cancer: more ore to be mined. Nat Rev Cancer 2013;13(05):342–355
33 Harada N, Kanayama M, Maruyama A, et al. Nrf2 regulates ferroportin 1-mediated iron efflux and counteracts lipopolysaccharide-induced ferroportin 1 mRNA suppression in macrophages. Arch Biochem Biophys 2011;508(01):101–109

34 Ursini F, Maiorino M. Lipid peroxidation and ferroptosis: the role of GSH and GPx4. Free Radic Biol Med 2020;152:175–185
35 Latunde-Dada GO. Ferroptosis: role of lipid peroxidation, iron and ferritinophagy. Biochim Biophys Acta, Gen Subj 2017;1861(08): 1893–1900
36 Maiorino M, Conrad M, Ursini F. GPx4, lipid peroxidation, and cell death: discoveries, rediscoveries, and open issues. Antioxid Redox Signal 2018;29(01):61–74
37 Song X, Wang X, Liu Z, Yu Z. Role of GPX4-mediated ferroptosis in the sensitivity of triple negative breast cancer cells to gefitinib. Front Oncol 2020;10:597434
38 Zou Y, Henry WS, Ricq EL, et al. Plasticity of ether lipids promotes ferroptosis susceptibility and evasion. Nature 2020;585(7826): 603–608
39 Raida Z, Hundahl CA, Nyengaard JR, Hay-Schmidt A. Neuroglobin over expressing mice: expression pattern and effect on brain ischemic infarct size. PLoS One 2013;8(10):e76565
40 Liu Y, Li B, Li Q, Zou L. Neuroglobin up-regulation after ischaemic pre-conditioning in a rat model of middle cerebral artery occlusion. Brain Inj 2015;29(05):651–657
41 Chen LM, Xiong YS, Kong FL, et al. Neuroglobin attenuates Alzheimer-like tau hyperphosphorylation by activating Akt signaling. J Neurochem 2012;120(01):157–164
42 Li RC, Pouranfar F, Lee SK, Morris MW, Wang Y, Gozal D. Neuroglobin protects PC12 cells against beta-amyloid-induced cell injury. Neurobiol Aging 2008;29(12):1815–1822
43 Xu WT, Xue YM, Wang C, et al. Effects of different frequencies of electric acupuncture stimulation on neuroglobin and NLRP3 signaling pathways in hematoma brain tissue in rats with cerebral hemorrhage. Mod J Integr Tradit Chin West Med 2022;31(01):10–15
44 Zhao X, Wang SS, Zhao NN, et al. Effect of Bushen Yisui Decoction combined with acupuncture on cognitive function improvement, cerebral hemodynamics and neuroglobin level of mild cognitive impairment after cerebral infarction. Liaoning Zhongyiyao Daxue Xuebao 2022;24(02):140–144
45 Nie YP. Effect of “Tongdu Tiaoshen” Acupuncture on Serum Neuroglobin Level in Patients with Cognitive Impairment After Ischemic Stroke and its Therapeutic Effect. Hefei: Anhui University of Chinese Medicine
46 Zheng SM, Lin XF. Up-regulation of electroacupuncture on the expression of neuroglobin in rats with septic encephalopathy. Chin J Clin Anat 2018;36(05):536–540
47 Yan H, He P, Wu ZH, et al. Effect of acupuncturing Dazhui, Baihui and Renzhong acupoints on expression of neuroglobin at different time points in Hippocampus of rats with cerebral ischemia reperfusion injury. J Hunan Univ Chin Med 2018;38(02):165–168
48 Wang J, Zhang W, Sun D, Song L, Li Y, Xu C. Analysis of neuroglobin mRNA expression in rat brain due to arsenite-induced oxidative stress. Environ Toxicol 2012;27(09):503–509
49 Jin K, Mao XO, Xie L, Khan AA, Greenberg DA. Neuroglobin protects against nitric oxide toxicity. Neurosci Lett 2008;430 (02):135–137
50 Yu Z, Poppe JL, Wang X. Mitochondrial mechanisms of neuroglobin's neuroprotection. Oxid Med Cell Longev 2013; 2013:756989
51 Shin JM, Lee KM, Lee HJ, Yun JH, Nho CW. Physalin A regulates the Nrf2 pathway through ERK and p38 for induction of detoxifying enzymes. BMC Complement Altern Med 2019;19 (01):101
52 Deshmukh P, Unni S, Krishnappa G, Padmanabhan B. The Keap1-Nrf2 pathway: promising therapeutic target to counteract ROS-mediated damage in cancers and neurodegenerative diseases. Biophys Rev 2017;9(01):41–56
53 Zhang F, Wang QW, Dai WB, et al. Anti-oxidative effect of Bidens biternata water extract on CCl4 induced acute liver injury in mice via Nrf2/Keap1 pathway. Drugs Clin 2023;38(04):755–760
54 Cai J, Yuan Y, Song JY, et al. Research on the action mechanism of antioxidant stress of Liuwei Dihuang Pill via Nrf2/HO-1 pathway in preventing and treating Alzheimer's disease. Modernization of Traditional Chinese Medicine and Materia Medica-World Science and Technology 2023;25(03):1002–1010
55 Solar Fernandez V, Cipolletti M, Ascenzi P, Marino M, Fiocchetti M. Neuroglobin As key mediator in the 17β-estradiol-induced antioxidant cell response to oxidative stress. Antioxid Redox Signal 2020;32(04):217–227
56 Zhang C, Hao X, Chang J, Geng Z, Wang Z. Mn-TAT PTD-Ngb attenuates oxidative injury by an enhanced ROS scavenging ability and the regulation of redox signaling pathway. Sci Rep 2019;9(01):20103
57 Zhang C, Yang R, Hao X, Geng Z, Wang Z. Mn-TAT PTD-Ngb ameliorates inflammation through the elimination of damaged mitochondria and the activation of Nrf2-antioxidant signaling pathway. Biochem Pharmacol 2020;178:114055